polymers

MDPI

Article

Flexural Strengthening of RC Slabs with Prestressed CFRP Strips Using Different Anchorage Systems †

José Sena-Cruz [1], Julien Michels [2,*], Yunus Emre Harmanci [2,3] and Luís Correia [1]

Received: date ; Accepted: date ; Published: date
Academic Editor: name

[1] Institute for Sustainability and Innovation in Structural Engineering (ISISE), Department of Civil Engineering, University of Minho, Guimarães 4800-058, Portugal
jsena@civil.uminho.pt (J.S.-C.); lcorreia@civil.uminho.pt (L.C.)
[2] Structural Engineering Research Laboratory, Empa, Swiss Federal Laboratories for Materials Science and Technology, Überlandstrasse 129, Dübendorf 8600, Switzerland
yunusemre.harmanci@empa.ch
[3] Department of Structural Mechanics, ETHZ, Swiss Federal Institute of Technology Zurich, Stefano-Franscini-Platz 5, Zürich 8093, Switzerland
* Correspondence: julien.michels@empa.ch; Tel.: +41-58-765-4139 Fax: +41-58-765-6955

† Correia, L., Texeira, T., Sena-Cruz, J., Michels, J.: Flexural Strengthening of RC Slabs with Prestressed CFRP strips using different Anchorage Systems, 7th International Conference on FRP Composites in Civil Engineering (CICE2014), Vancouver (BC, Canada), 2014

Abstract: Externally Bonded Reinforcement (EBR) technique has been widely used for flexural strengthening of concrete structures by using carbon fiber-reinforced polymers (CFRP). EBR technique offers several structural advantages when the CFRP material is prestressed. This paper presents an experimental and numerical study on reinforced (RC) slabs strengthened in flexure with prestressed CFRP strips as a structural strengthening system. The strips are applied as an externally bonded reinforcement (EBR) and anchored with either a mechanical or a gradient anchorage. The former foresees metallic anchorage plates fixed to the concrete substrate, while the latter is based on an accelerated epoxy resin curing followed by a segment-wise prestress force decrease at the strip ends. Both anchorage systems, in combination with different CFRP strip geometries, were subjected to static loading tests. It could be demonstrated that the composite strip's performance is better exploited when prestressing is used, with slightly higher overall load carrying capacities for mechanical anchorages than for the gradient anchorage. The performed investigations by means of a cross-section analysis supported the experimental observation that in case a mechanical anchorage is used, progressive strip debonding changes the fully bonded configuration to an unbonded end-anchored system. The inclusion of defined debonding criteria for both the anchorage zones and free length between the anchorage regions allowed to precisely capture the ultimate loading forces.

Keywords: RC plate strengthening; CFRP strips; prestressing; mechanical anchorage; gradient anchorage; static loading tests; cross-section analysis; numerical simulations

1. Introduction

In recent decades, several research initiatives has been devoted to the development of Fibre Reinforced Polymer (FRP) materials and related strengthening techniques used by the construction industry [1–8]. Nowadays, these materials and strengthening techniques are relatively well-unknown by researchers, designers and constructors being, respectively, for the case of retrofitting concrete structures the Carbon FRP materials (CFRP) and the externally bonded reinforcement (EBR) technique the most used ones. Epoxy adhesives are typically used as bond agent. In some specific applications, the use of prestressed FRP materials is appropriate or even required [9–15]. This alternative technique combines the benefits of the passive EBR FRP systems with the advantages associated with external prestressing. El-Hacha *et al.* [16] pointed out the following main advantages: (1) superior durability since non-corrosive materials are used; (2) the existing deflections are reduced; (3) the crack widths reduction and the onset of cracking initiation is delayed; (4) internal steel reinforcement strains are relieved; (5) higher fatigue failure resistance; (6) more efficient use of the concrete and FRP; (7) opposes stresses due to both dead and live loads; (8) ultimate capacity can be further increased; (9) it can be worked as a substitute of internal pre-stress that has been lost; (10) shear capacity is increased by the longitudinal stresses induced by prestressed FRP laminates. Mainly three systems have been proposed to prestress the FRP materials [16]: (1) cambered prestressing systems; (2) prestressing against an independent element; and (3) prestressing against the element to be strengthened. Up to now the systems that apply the prestressing against the element to be strengthened are the most used, due to their main advantages in terms of practicality. At the ends of the prestressed FRP elements special end-anchorage systems are required in order to transfer the high shear stress developed from the reinforcing material into the concrete substrate in order to avoid a premature FRP peeling-off failure. From all the proposed systems, two of them have been mostly used, mainly [17]: the mechanical anchorage (MA) system fixing the ends of the FRP reinforcement to the concrete substrate by means of metallic plates and bolts and the gradient anchorage (GA). Detailed information about these two systems is given in Section 2.3.

To assess to the performance of the mechanical and gradient anchorage systems, an experimental program was carried out. In addition to the study of anchorage systems (MA and GA), the cross-section geometry of the CFRP laminate strip was also investigated. For that purpose, eight reinforced concrete (RC) slabs, strengthened with pre-stressed CFRP laminate strips and anchored according

the to the MA and GA systems, were monotonically tested under displacement control up to failure by using a four-point bending test configuration. The observed performance of the tested RC slabs is presented and critically analyzed. Additionally, by using a cross-sectional analytical model, numerical simulations were carried out to better understand the obtained results with regard to the overall structural behavior. This calculation tool is able to predict the structural behavior of RC structures strengthened with an additional reinforcement. This external reinforcement can be implemented as either a fully bonded or an unbonded strengthening element.

2. Experimental Program

2.1. Test Program

The experimental program was composed of eight reinforced concrete (RC) slabs, as presented in Table 1: (1) two slabs were used as reference specimens (REF1 and REF2); (2) one slab (SL50_1.4_EBR) was strengthened with one laminate according to the externally bonded reinforcement (EBR) technique; (3) five slabs were strengthened with one EBR prestressed CFRP laminate strip, three by using the mechanical anchorage (MA) system and two with the gradient anchorage (GA) system, with distinct geometry types of CFRP laminate strips, mainly 50 mm × 1.4 mm, 50 mm × 1.2 mm, and 80 mm × 1.2 mm. The CFRP strip prestrain $\varepsilon_{f,p}$ was measured with strain gauges installed at its mid-length.

Table 1. Experimental program (b_f = strip width, t_f = strip thickness, $\varepsilon_{f,p}$ = strip prestrain, f_{cm} = average compressive strength on cylinder of concrete at slab testing day, E_{cm} = average Young's modulus of concrete at slab testing day; the values between parentheses are the corresponding coefficients of variation (CoV)).

Slab	CFRP Strip ($b_f \times t_f$)	Anchorage	$\varepsilon_{f,p}$ (‰)	f_{cm} (MPa)	E_{cm} (GPa)
REF1	-	-	-	53.4 (4.3%)	32.2 (7.5%)
REF2	-	-	-	57.4 (3.0%)	32.6 (0.1%)
SL50_1.4_EBR	50 mm × 1.4 mm	-	-	53.4 (4.3%)	32.2 (7.5%)
SL50_1.4_MA	50 mm × 1.4 mm	MA	3.98	53.4 (4.3%)	32.2 (7.5%)
SL50_1.4_GA	50 mm × 1.4 mm	GA	4.05	53.4 (4.3%)	32.2 (7.5%)
SL50_1.2_MA	50 mm × 1.2 mm	MA	4.19	49.5 (3.1%)	n.a.
SL80_1.2_MA	80 mm × 1.2 mm	MA	3.99	57.4 (3.0%)	32.6 (0.1%)
SL80_1.2_GA	80 mm × 1.2 mm	GA	4.06	57.4 (3.0%)	32.6 (0.1%)

The specimens' geometry and test configurations are shown in Figure 1. The RC slabs have a total length of 2600 mm and rectangular cross section of 600 mm (width) by 120 mm (depth). In the tension region, the slabs are reinforced with 5

longitudinal steel bars of 8 mm of diameter (5⌀8), whereas in the compression zone 3⌀6 are used. Secondary and transverse reinforcement is also used composed of closed steel stirrups of ⌀6 at 300 mm spacing.

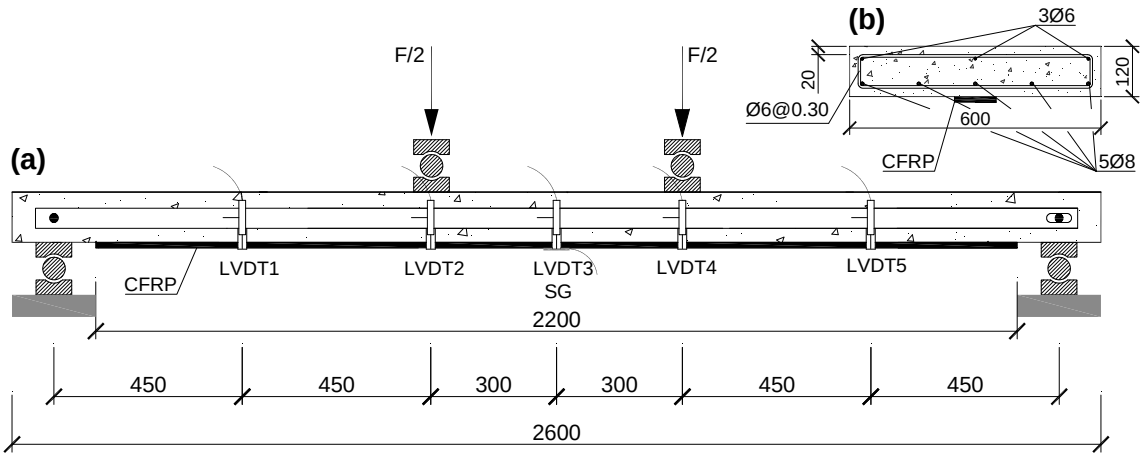

Figure 1. Slab geometry and testing configuration (all units in (mm)).

All the slabs were monotonically tested up to the failure, by using a servo-controlled equipment under midspan displacement control at a rate of 1.2 mm/min. Four point bending test configuration was used. Instrumentation includes: (1) 5 linear variable differential transducers (LVDT1 to LVDT5) to measure the displacements along the slab's longitudinal axis; (2) a TML BFLA-5-3 strain gauge sensor (SG) to record the CFRP strain at its mid-length; and (3) a load cell to measure the applied load F. Figure 1 shows the position of the five displacement transducers: three (LVDT2 to LVDT4) in the pure bending zone with the range of ±75 mm and a linearity error of ±0.10% and two (LVDT1 and LVDT5) between the supports and the applied load points with a range of ±25 mm and the same linearity error. The load cell, with a maximum measuring capacity of 200 kN and a linear error of ±0.05%, was placed between the actuator and the steel device that distributed the load into equal parts (see Figure 1).

2.2. Materials

The material characterization included the evaluation of the mechanical properties of concrete, steel, CFRP laminate strips and epoxy adhesive.

Three batches were used to cast the RC slabs. Six cylindrical concrete specimens with 150 mm of diameter and 300 mm of height of each concrete batch were used to evaluate the modulus of elasticity and compressive strength through the LNEC E397-1993:1993 [18] and NP EN 12390-3:2011 [19] recommendations, respectively. These tests were performed at the same age than for the static tests of the slabs. An average compressive strength of about 53.4 MPa was obtained, see Table 1. The tensile properties of the steel reinforcement were evaluated using the standard NP

EN ISO 6892-1:2012 [20]. Three specimens with 500 mm of length were used for each bar type. To measure the strains during the linear branch of the stress-strain curve, a clip gauge with a 50 mm of initial length was used. Figure 2 shows the relationship between the tensile stress and displacement between grips, whereas Table 2 includes the obtained results in terms of Young's modulus E_s, yielding strength $f_{s,y}$, and ultimate tensile strength $f_{s,u}$. In spite of both bar types presented similar Young's modulus, Figure 2 shows a yielding plateau and lower values in terms of $f_{s,y}$ and $f_{s,u}$ for the case of a ⌀8 bar.

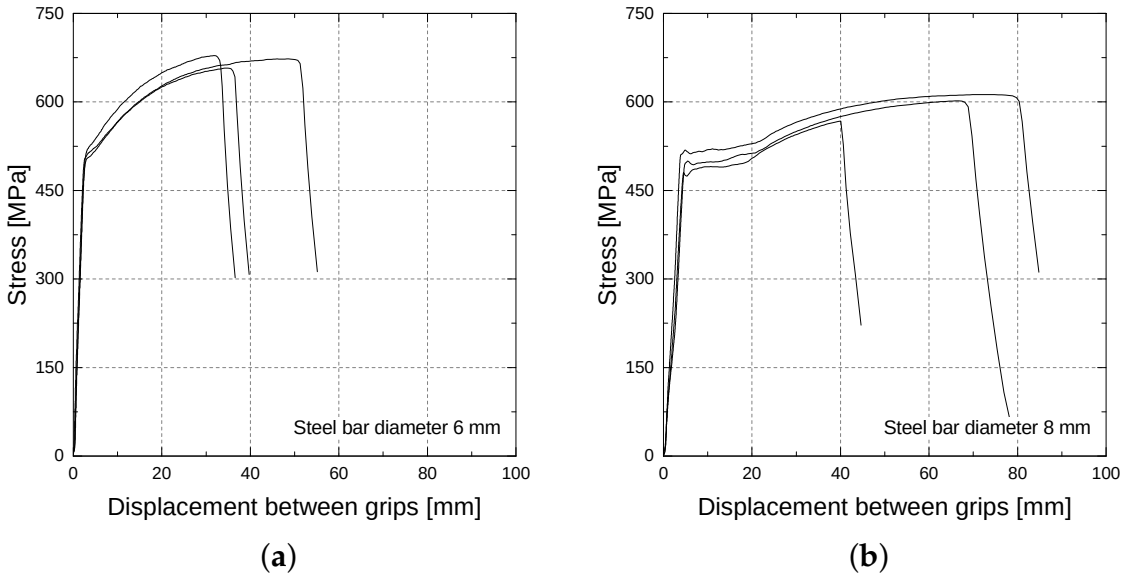

Figure 2. Tensile stress *vs.* displacement between grips of **(a)** ⌀6 steel bar; **(b)** ⌀8 steel bars.

Table 2. Tensile properties of the reinforcing steel bars.

Bar Type (⌀in (mm))	E_s **(GPa)**	f_y **(MPa)**	$f_{s,u}$ **(MPa)**
⌀6	209.5 (8.5%)	579.3 (3.3%)	669.7 (1.7%)
⌀8	212.8 (9.7%)	501.4 (5.9%)	593.9 (3.9%)

The CRFP laminate strips (Type: *S&P Laminates CFK*) used in the present experimental program are prefabricated (pultruded) and consist of unidirectional carbon fibers held together by an epoxy vinyl ester resin matrix. This composite material is provided in rolls of 150 m total length, has a smooth external surface and a black appearance. Tensile properties were assessed throughout ISO 527-5:1997 [21] recommendations. Four samples were used for each CFRP section type. A clip gauge with 50 mm of initial length was used to measure the strains. Table 3 presents the obtained results in terms of Young's modulus E_f and ultimate tensile strength $f_{f,u}$.

Table 3. Mechanical properties of the CFRP strips.

Geometry (mm × mm)	E_f **(GPa)**	$f_{f,u}$ **(MPa)**
50 × 1.2	167.7 (2.9%)	2943.5 (1.6%)
50 × 1.4	154.8 (4.6%)	2457.1 (1.2%)
80 × 1.2	164.6 (0.2%)	2455.3 (5.0%)

The two-component epoxy adhesive (Type: *S&P Resin 220*) was used to bond the CFRP laminate strips to the concrete substrate. This epoxy adhesive is a solvent free, thixotropic and grey two-component (Component A = resin, light grey color and Component B = hardener, black color). The tensile properties of this epoxy adhesive was assessed following the ISO 527-2:1993 [22]. The specimens were cured with similar conditions to the ones that are used with mechanical (MA) and gradient (GA) anchorage systems (Michels *et al.*, 2013 [17]). Six and four specimens were tested in each series, and were cured during 7 and 3 days, respectively, for the MA and GA. The difference in age of the epoxy at the testing date is explained by the different necessary curing time in order to reach a more or less stable tensile strength and stiffness. For the GA, the epoxy resin undergoes accelerated curing at high temperatures, and hence already develops significant strength and stiffness during the anchorage application. For the MA, however, the epoxy resin undergoes normal curing at room temperature and is hence delayed in strength and stiffness development compared to the resin with an initial accelerated curing. Detailed studies on strength development of epoxy resins under different curing conditions can be found in Moussa *et al.* [23]. Figure 3 shows the stress-strain relationships from the tests carried out. Secant modulus of elasticity was defined using the two points with 0.05% and 0.15% of strain, being the average values equal to 8.68 GPa (CoV = 5.7%) and 5.79 GPa (CoV = 9.5%) for the case of MA and GA, respectively. Finally, the obtained average tensile strength was equal to 20.72 MPa (CoV = 18.25%) and 14.85 MPa (CoV = 11.28%) for the MA and GA, respectively.

2.3. End-Anchorage

2.3.1. Anchorage Systems

As mentioned before, two distinct end-anchorage systems were investigated: (1) the mechanical anchorage (MA), which uses metallic plates at the ends of the FRP strips, and (2) the gradient anchorage (GA), which is produced by sector-wise heating of the adhesive and a step-wise releasing of the prestressed force F_p. The studied commercial systems, available from the same supplier as for the CFRP reinforcement and adhesive, present several common and specific equipment. These are presented in Figure 4. The MA system uses metallic anchor plates of 200 mm × 272 mm × 12 mm fixed with 6 M16 8.8 bolt anchors, guides, clamp units, frames, hydraulic hoses and cylinders, and a manual hydraulic pump. For the

case of the GA system, guides, clamp units, frames, hydraulic hoses and cylinders, manometer and valves, and heating device for accelerated curing the adhesive, are required. Depending on the level of prestressing to be applied and the length of the CFRP laminate strip to be prestressed, the MA can have one or both active anchorages. In the case of the GA system both anchorages are active. Regarding the duration of the strengthening application, in the MA system all the steps are concluded after approximately 24 h, whereas for the case of GA only 3 to 4 h are required. In the MA a significant cure of the epoxy adhesive along the CFRP laminate is required, which takes in normal conditions at about 24 h (Granja *et al.* [24]). Since the GA system uses the adhesive's ability to cure fast at high temperatures, significant lower period of time is needed to conclude the strengthening application. More detailed information about the accelerated curing properties of commercially available adhesives are listed in Czaderski *et al.* [25] and Michels *et al.* [26]. Finally, at the end in the case MA system in addition to the CFRP laminate strips two metallic anchors will exist, while for the case of the GA system the strengthening solutions will be composed by a purely bonded CFRP strip/epoxy/concrete system.

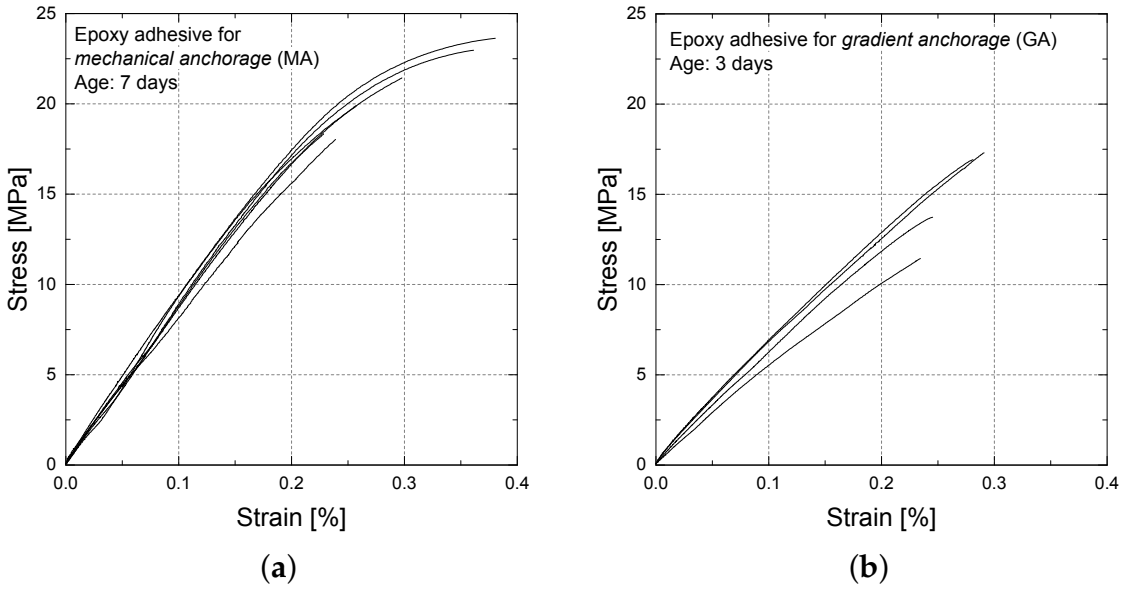

Figure 3. Tensile stress *vs.* strain of epoxy adhesive used with Epoxy adhesive for MA; (**b**) Epoxy adhesive for GA.

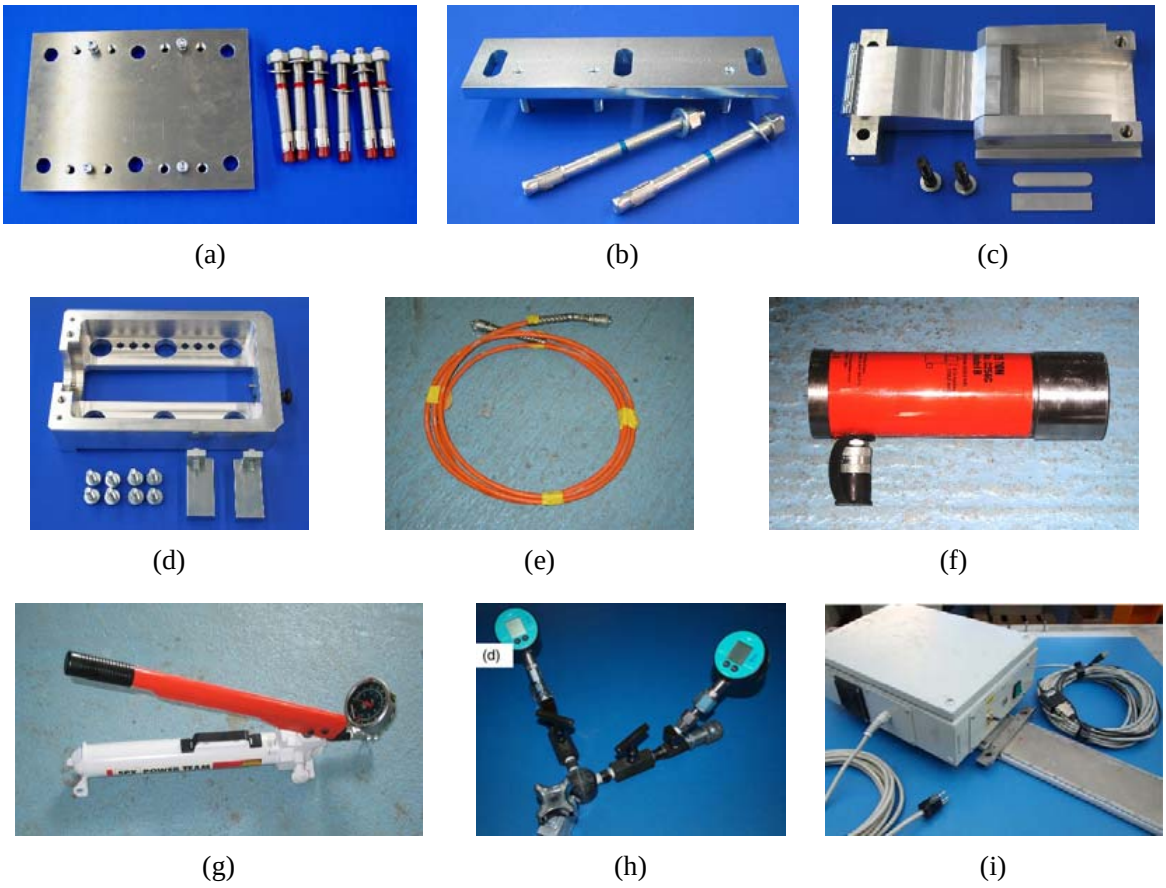

Figure 4. Equipment composing the anchorage systems: (**a**) metallic plate anchors (MA); (**b**) guides (MA&GA); (**c**) clamp unit (MA&GA); (**d**) frame (MA&GA); (**e**) hydraulic hoses (MA&GA); (**f**) hydraulic cylinder (MA&GA); (**g**) manual hydraulic pump (MA&GA); (**h**) manometer and valves (GA); (**i**) heating device (GA).

2.3.2. Strengthening Procedure

Figure 5a,b schematically present the main steps for the strengthening using the MA and GA systems, respectively, mainly:

(A) The first step consists on surface preparation of the slabs where the CFRP laminate strip will be applied. In the present case a grinding stone wheel is used. Subsequently, compressed air was used to clean the treated region.
(B) Several holes are drilled to accommodate temporary and permanent bolt anchors. GA system complies only temporary bolts, while for the case of MA system, six M16 8.8 permanent bolt anchors are used to fix each metallic anchorage plate. The HIT-HY 200-A® chemical bond agent was used to fix these bolts to concrete. Then, aluminium guides are placed in the right position to guide and fix the clamp units. Afterwards the clamp units are placed in its position, *i.e.*, in-between the guides at each extremity of the slab.

(C) The CFRP laminate strip is cleaned with a solvent and the epoxy adhesive is prepared according to the information given by the producer's technical datasheet. It should be remarked that before this step, the CFRP laminate strip had been already instrumented with a strain gauge at its mid-length (see also Section 2.1). Subsequently, the adhesive is applied on the surface of the CFRP laminate as well as on the concrete surface region in contact with the laminate. The CFRP laminate strip is then placed in its final position and slightly pressed against the concrete substrate. In the end a minimum of 2 mm of thickness of epoxy is assured. The clamp units are installed in-between the guides at each extremity of the slab and are closed to fix the CFRP laminate strip.

(D) For the case of MA system, metallic anchor plates are slightly grinded with sandpaper and cleaned with a solvent before they are installed in their predefined location. In the case of GA, heating devices are placed in the gradient zone.

(E) The aluminium frames are then placed on their predefined locations and fixed against the concrete with the bolt anchors in order to accommodate the hydraulic cylinder.

(F) Eventually, the hydraulic cylinder cylinders are installed in the aluminium frame and using a manual hydraulic pump, the prestress is applied to the CFRP laminate strip.

After prestressing the CFRP, distinct procedures are followed for the case of the MA and the GA systems. For the case of the MA system, in order to increase the confinement provided by the metallic anchor plates at the anchor's region and consequently reduce the probability of the CFRP laminate sliding at the ends, a torque of 150 N·m is applied in the six bolt anchors. Additional fixing screws mounted in-between the frame and the clamp units are used to block the prestressing system in order to avoid pre-stress losses during the curing of the epoxy. As referred before, the strengthening application is concluded after approximately 24 h. In the end, all the equipment is removed and the temporary bolt anchors and CFRP laminate outside of the anchor plates are cut off.

For the case of the GA system, in the ambit of the present experimental program, a 600 mm anchorage length was used, composed of three sectors (50/80 mm wide and 200 mm long each). During the application of the gradient, the specimens are always monitored in terms of applied force by the hydraulic cylinders and temperature at the distinct sectors composing the heating devices. Details about the evolution of the temperature inside the epoxy adhesive in the respective sectors during the application of the gradient can be found in Michels *et al.*, 2013 [17]. Generally, the aimed epoxy temperature T_a is about 90 °C. The releasing force in each sector was equal to about 1/3 of the total applied force F_p. The total heating duration was 35 min with the subjected temperature profile of the heating elements T_h as shown in Figure 6 for both strips 50 mm × 1.4 mm and 80 mm × 1.2 mm. Each force release ΔF was performed approximately 15 min after the initiation of the

cooling phase of the corresponding sector. This waiting time was chosen in a way to ensure that the epoxy adhesive has cooled down to temperatures below 50 °C.

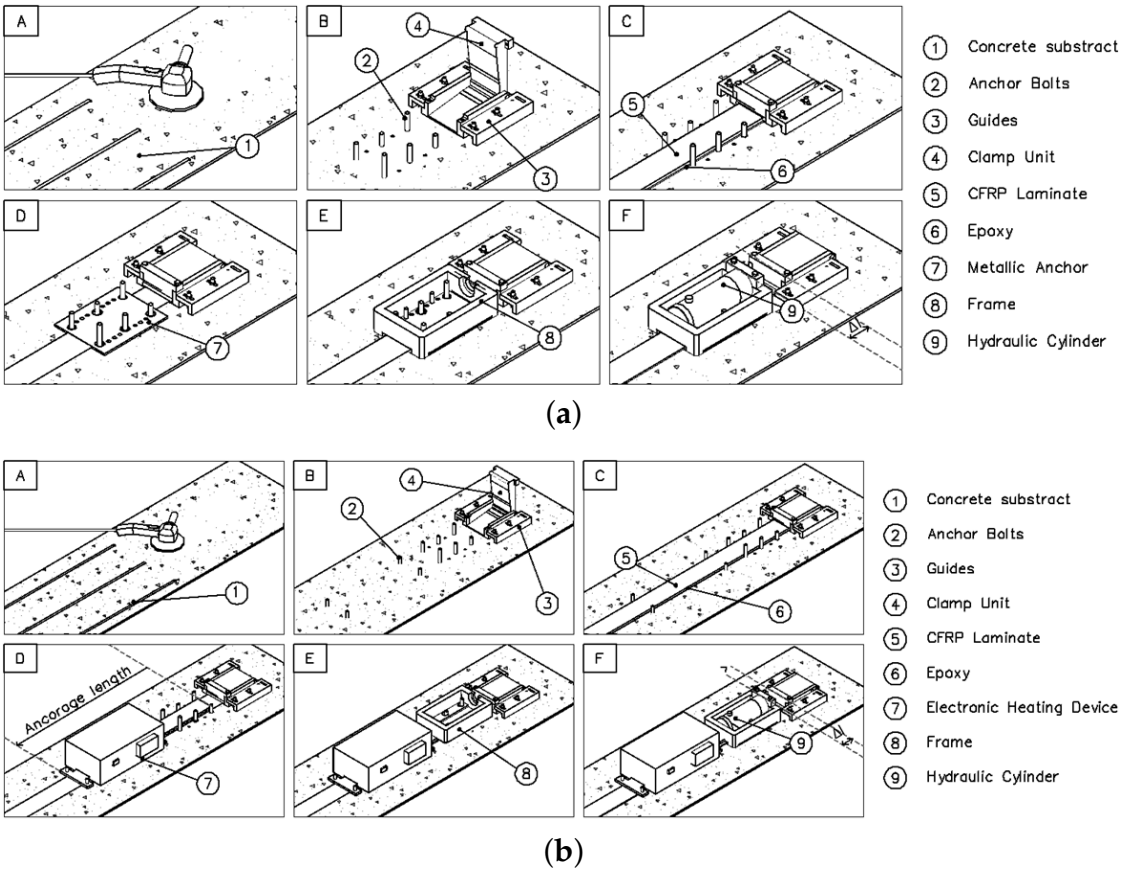

Figure 5. Application procedures for MA and GA systems, (**a**) Mechanical Anchorage; (**b**) Gradient Anchorage.

As previously mentioned, in each single prestressed slab a strain gauge was installed on the at midspan of the CFRP laminate strip to control the prestrain level $\varepsilon_{f,p}$ to be applied during the strengthening phase and to record the strains attained during the monotonic test up to the failure. The CFRP laminate strip was prestrained to an average value of more or less 0.4%. Table 1 includes the values of the registered prestrain at the middle of the laminate at the end of the strengthening. The specimens were kept in lab environment after strengthening at least one month prior to testing.

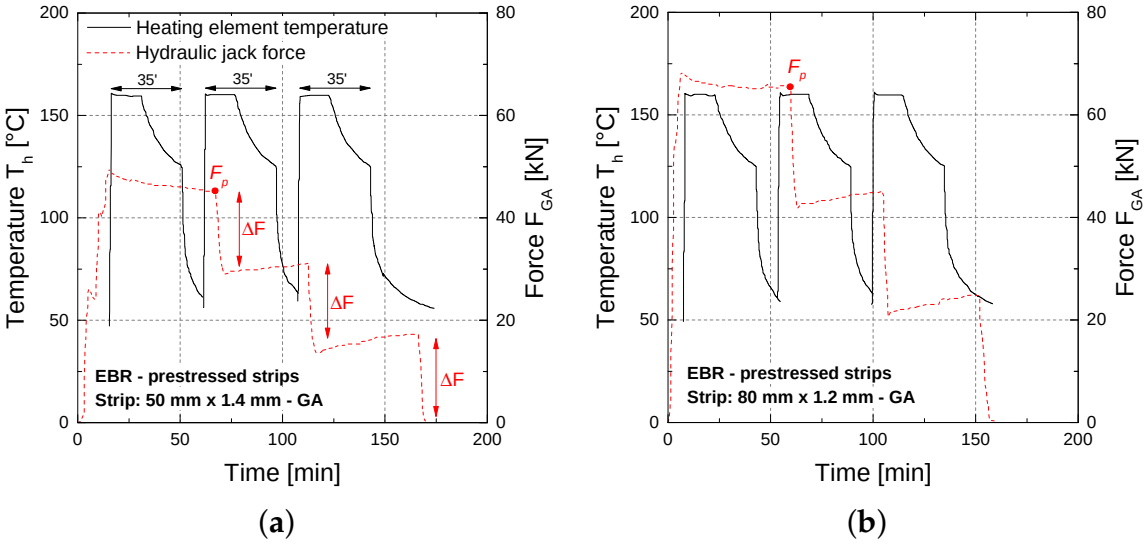

Figure 6. Heating element temperature T_h and gradient force F_{GA} evolution over time. (**a**) 50 mm × 1.4 mm strip; (**b**) 80 mm × 1.2 mm strip.

3. Numerical Investigation

3.1. Cross Section Analysis (CSA)

Cross-Section Analysis (CSA) was performed with a Matlab-based calculation tool. The differences in strain distribution between *bonded* and *unbonded* external reinforcements are given in Figure 7. For *bonded* configurations, conventional force equilibrium and strain compatibility in the cross-section can be considered. After establishing the moment-curvature (M,κ)-relation, deflection values can afterwards simply be derived by double integration of the curvature over the span length. For *unbonded* configurations, however, strain compatibility between the CFRP tensile strain and the bottom concrete surface is not given anymore. In this case, CFRP tensile strain ε_f, which is for each loading step constant over the whole strip length L, has to correspond to the average concrete tensile strain $\varepsilon_{c,bot,avg}$ at the bottom for each loading step:

$$\varepsilon_f = \frac{1}{L} \cdot \int_0^L \varepsilon_{c,bot}(x) \cdot dx = \varepsilon_{c,bot,avg} \tag{1}$$

Such a condition requires a much more complex calculation procedure, implicating iteration procedures for the cross-section analysis on several locations over the whole span lengths and afterwards a verification of the CFRP tensile strain and average concrete bottom strain compatibility. Tension stiffening has been included through the *tension chord model* by Marti *et al.* [27]. The exact calculation

procedure with a vectorized optimization approach can be found in Harmanci [28] and Harmanci *et al.* [29].

3.2. Debonding Failure Modes

In addition to the listed material failures in compression (concrete) and tension (concrete, steel, CFRP), several debonding criteria have been included in the cross-section analysis in order to precisely assess the ultimate load carrying capacity.

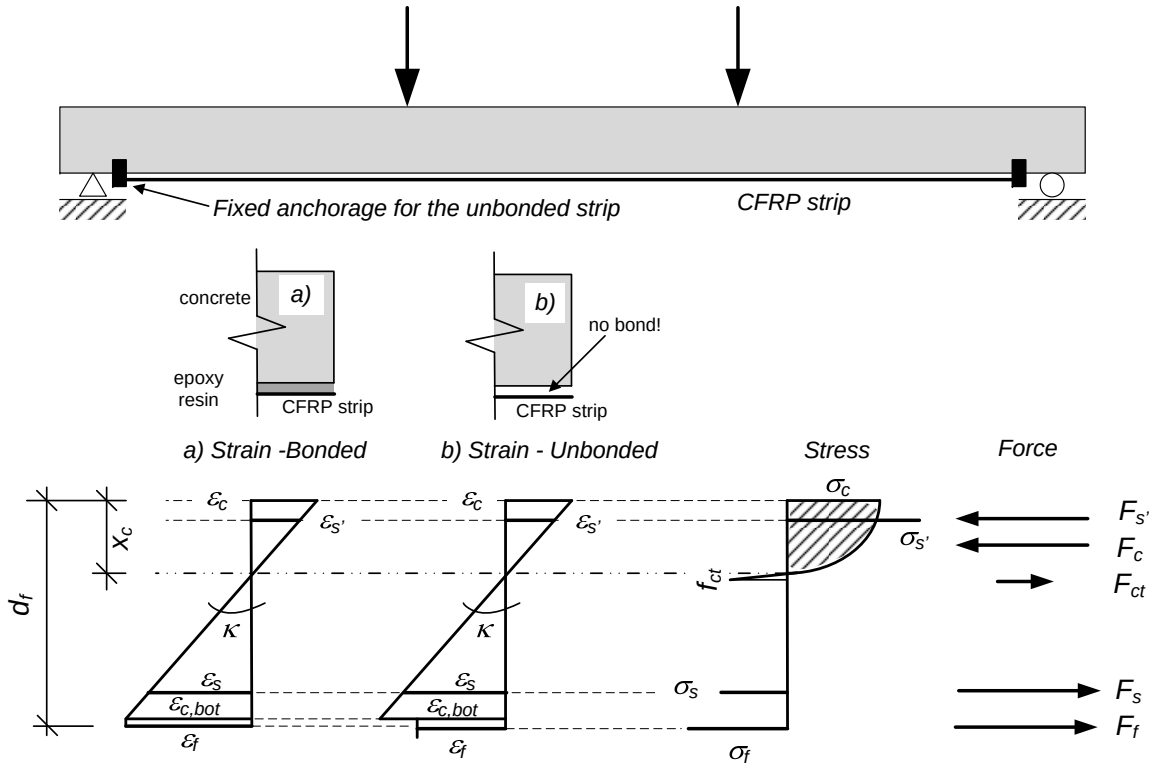

Figure 7. Differences in strain distribution for a bonded and unbonded CFRP/concrete system configuration.

3.3. Constitutive Material Laws

The different materials have been implemented as shown in Figure 8. Concrete was defined linear elastic up to failure in tension, and by a Hognestad parabola in compression [30]. Reinforcing steel was considered elastic-plastic with a simple bi-linear law, and eventually CFRP was modelled linear-elastic up to unidirectional tensile failure.

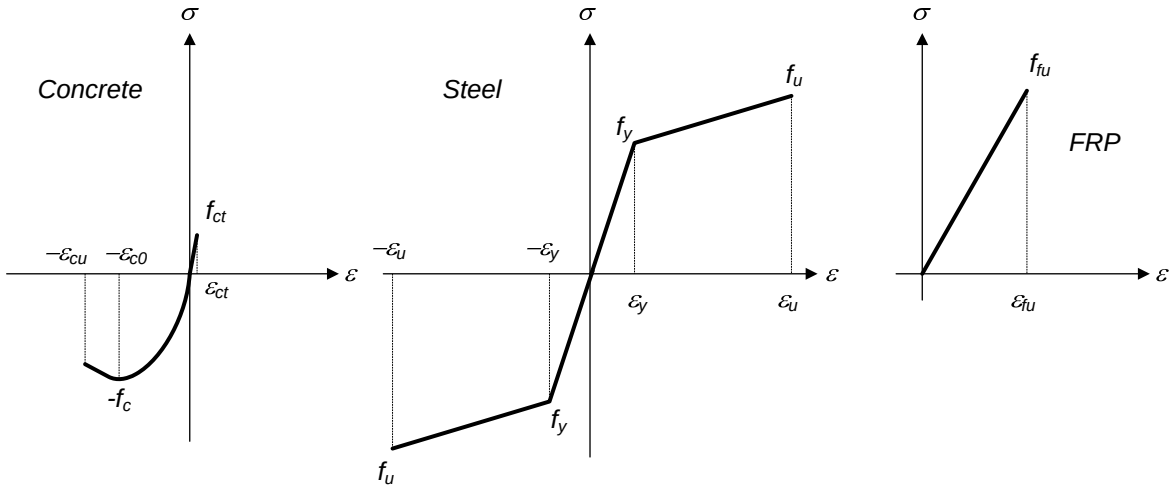

Figure 8. Constitutive material laws for concrete, steel, and CFRP.

1. For initially unstressed EBR, the debonding modes listed in the Swiss design recommendations SIA166 [2] have been used. These include:
   - *End-anchorage failure* (DM1, with: $F_{f,cr}$ being the CFRP strip force at the last crack, F_R being the anchorage resistance):

$$F_{f,cr} < F_R \tag{2}$$

   - *Intermediate strip debonding due to interfacial shear stress exceeding* (DM2, limit value for the shear strength τ_{lim} being a function of the concrete tensile strength):

$$\tau < \tau_{lim} \tag{3}$$

   - *Intermediate strip debonding due to CFRP strip strain exceeding* (DM3):

$$\varepsilon_f < 8‰ \tag{4}$$

2. For prestressed CFRP strips, design criteria for the gradient anchorage failure defined in the PhD thesis of Czaderski [31] have been included.
3. For prestressed CFRP strips with a mechanical anchorage (Type: S&P Clever Reinforcement Company AG), an upper limit for the CFRP strip strains ε_f of at maximum 10‰ at the anchorage start have been implemented. This value is based on suggestions given by Suter and Jungo [32].
4. For both prestressed configurations with either a gradient or a mechanical anchorage, the intermediate strip debonding as defined in the SIA166 [2] have also been incorporated. The strip strain limitation was based on the additional strip strain $\Delta\varepsilon_f$ (Verification: $\Delta\varepsilon_f < 8‰$). The applicability to prestressed systems has been demonstrated in Harmanci [33].

4. Results and Discussion

4.1. General Comments

Experimental load-midspan deflection curves are presented in Figure 9, and in Figure 10 along with the numerical simulations. All characteristic results for the cracking "*cr*", yielding "*y*", and ultimate loading state "*u*" are presented in Table 4. Additionally, the structural ductility with the ductility index for deflection μ_δ as well as the strength factor μ_F as defined in Michels *et al.* [15] are given. As expected, the strengthened slabs (EBR, GA and MA specimens) exhibit higher cracking, yielding, and ultimate loads but lower deflections at failure compared to the reference slabs REF1 and REF2.

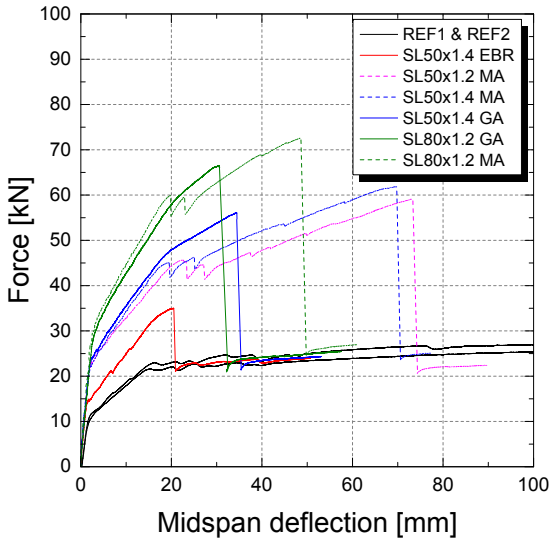

Figure 9. Experimental load-deflection curves.

4.2. Failure Modes

The reference slab tests were stopped at a midspan deflection of 100 mm due to the corresponding LDVT measurement range limitation. Failure mode would in this case most likely be concrete crusing on the top fiber. The strengthened slabs all exhibited CFRP strip debonding, which occured partially in the concrete substrate or in the CFRP/epoxy or epoxy/concrete interface. Debonding mostly initiated at one slab extremity and then propagated towards the other support. For the slabs with a mechanical end-anchorage, strip debonding did not implicate the immediate reaching of the ultimate load carrying capacity, since the strip was still held at its both ends. Further load increase was still possible. Eventually, the strip was pulled out of the mechanical anchorage as shown in Figure 11. Details regarding the structural behavior will be discussed in the next sections. The slabs with gradient anchorage exhibited a more sudden strip debonding, as in this case no mechanical end-fixing could provide additional anchorage resistance.

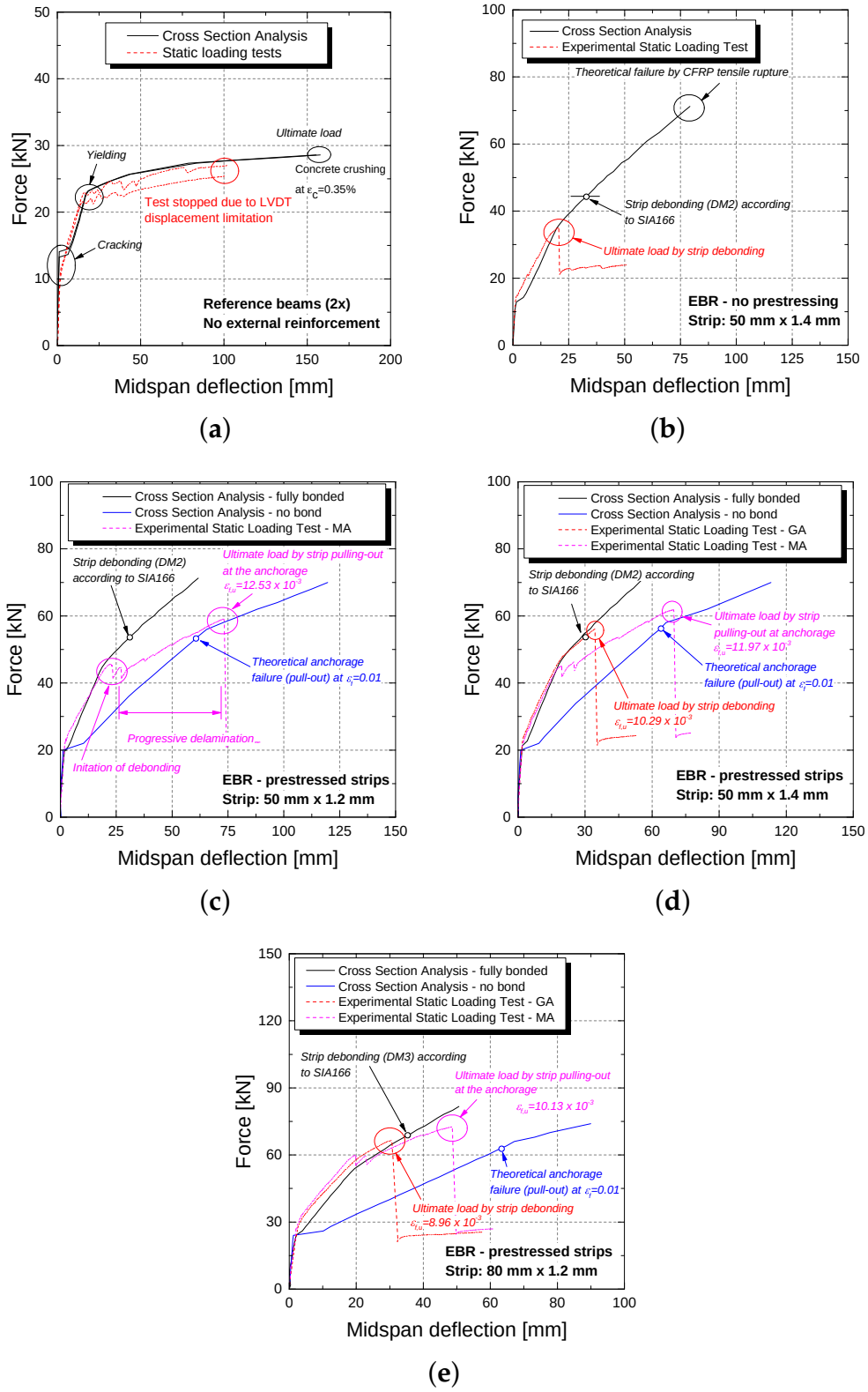

Figure 10. Experimental and Numerical force-deflection comparison for all slabs. (**a**) Reference slabs; (**b**) EBR—No prestressing; (**c**) Prestessed strip—50 mm × 1.2 mm; (**d**) Prestessed strip—50 mm × 1.4 mm; (**e**) Prestessed strip—80 mm × 1.2 mm.

Table 4. Key experimental results (δ_{cr} = deflection at crack initiation, F_{cr} = cracking load, δ_y = deflection at yielding, F_y = yielding load, δ_u = ultimate deflection, F_u = ultimate load, $\varepsilon_{f,u}$ = CFRP tensile strain at failure, μ_δ = ductility index, $\mu_F = F_u/F_y$ = strength factor).

Plates	δ_{cr} (mm)	F_{cr} (kN)	δ_y (mm)	F_y (kN)	δ_u (mm)	F_u (kN)	$\varepsilon_{f,u}$ (‰)	Failure Mode	$\mu_\delta = \delta_u/\delta_y$	$\mu_F = F_u/F_y$
REF1	2.47	11.04	15.74	21.5	-	-	-	-		
REF2	2.49	11.12	15.96	22.9	-	-	-	-		
SL50x1.4_EBR	1.64	14.73	17	33.3	20.47	35.06	4.64	Strip debonding	1.20	1.05
SL50x1.4_GA	2.25	23.84	18.86	48.35	34.39	56.02	10.29	Strip debonding	1.82	1.16
SL50x1.4_MA	2.25	22.07	17.8	44.32	69.84	61.76	11.97	Strip pulled out of mech. anchorage	3.92	1.39
SL50x1.2_MA	2.53	22.81	20.57	44.89	73.23	59.09	12.53	Strip pulled out of mech. anchorage	3.56	1.32
SL80x1.2_GA	2.88	28.56	20.31	58.31	30.61	66.21	8.96	Strip debonding	1.51	1.14
SL80x1.2_MA	2.51	28.71	18.43	58.67	48.62	72.58	10.13	Strip pulled out of mech. anchorage	2.64	1.24

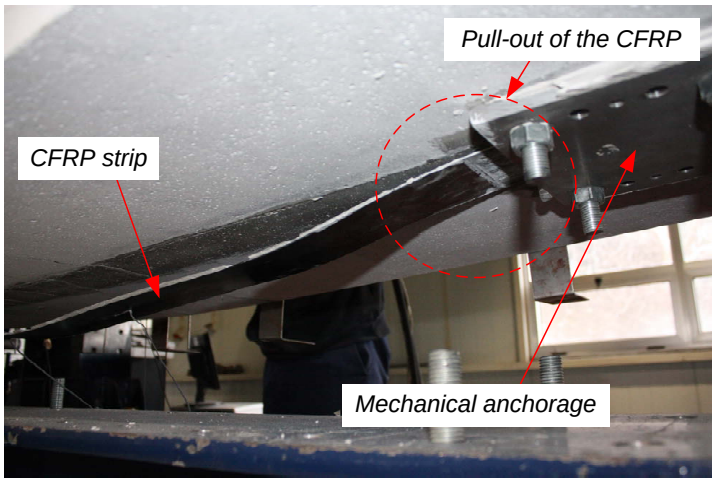

Figure 11. CFRP strip pull-out from the mechanical end-anchorage.

4.3. Prestressed versus Non-Prestressed

As expected, the use of prestressing improved the overall structural behavior of the slabs in terms of cracking and yielding initiation, stiffness, and load carrying capacity compared to a simple EBR solution (Figure 9 and Figure 10a,b). Although the initial stiffness in the uncracked stage did not change significantly, mainly due to the low level of strengthening, cracking load is significantly higher (almost doubled with a 50 mm $\times$ 1.4 mm prestressed strip compared to only 33% with an unstressed one). Similar observations can be made for overall stiffness prior to yielding. The ultimate load increase is between about 25% for en EBR strips and between 100 and 120% for the prestressed configurations with gradient and mechanical anchorage, respectively. Finally, it should be also referred that prestressing also better explores the CFRP's mechanical properties in tension. The measured ultimate CFRP strains $\varepsilon_{f,u}$ were 10.29 and 11.97‰ in case the laminates were prestressed, but only 4.64‰ could be used with an initially unstressed strip (Table 4). Additionally, as presented in Table 4, a better structural behavior in terms of ductility can be noticed when a prestressed EBR with a MA is applied. A relative improvement of about 68% in ultimate deflection was observed, while the deflection at yielding is almost identical. This also results in a much higher ductility index μ_δ. In terms of load, the prestressed EBR system with MA also exhibits a more distinct load carrying improvement after the yielding initiation.

4.4. Gradient Anchorage (GA) vs. Mechanical Anchorage (MA)

Up to yielding initiation, GA and MA systems exhibited similar behavior (Figure 10d,e). From this point on, additional contribution provided by the steel reinforcement is limited, the CFRP strip being now responsible to carry additional load. This is the reason why the force increment carried by CFRP material drastically increases at the onset of yielding initiation (Figure 12). For all MA slabs, two drop

points can be observed just after yielding initiation. These two drops are related to a strip debonding initiation at the both extremities (in between the metallic plate anchors). After this point the slab still continues to carry load due to the existence of the metallic anchors that avoided the premature debonding of the CFRP laminate strip. For this reason, the slabs of MA series present a better performance in terms of ultimate load when compared with the GA series, for which the initial debonding process is rapidly transformed into the complete strip detachment. In Table 4, it can be seen that the ultimate loads reached with a mechanical anchorage are about 10% higher than for a gradient anchorage. Deflection at failure, is around 103% (50 mm $\times$ 1.4 mm) and 59% (80 mm $\times$ 1.2 mm) higher for a mechanical anchorage compared to a purely bond-based gradient anchorage. In terms of structural ductility, both times the MA exhibit a more favorable behavior with ductility indexes of 3.92 and 2.64 for the strip section 50 mm $\times$ 1.4 mm and 80 mm $\times$ 1.2 mm, respectively. The same is valid for the additional force increase after yielding initiation.

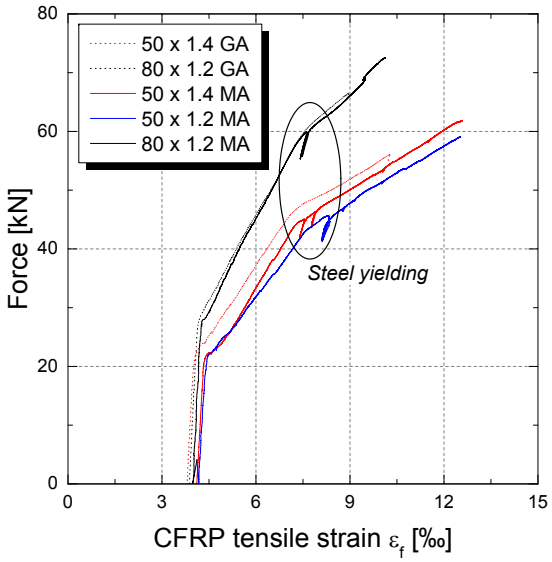

Figure 12. Experimental CFRP tensile strains in function of the applied load.

4.5. Influence of FRP Thickness t_f *and Width* b_f

As shown in Figure 10c,d, SL50x1.2_MA and SL50x1.4_MA slabs presented a relatively similar behavior, with eventually a slightly higher ultimate load for the thicker laminate (61.8 kN against 59.09 kN). Considering the measured strains at failure listed in Table 4 together with the elastic moduli for both strip thicknesses, the pull-out forces are in both cases very close (see Figure 13): 126 kN for $t_f = 1.2$ mm and 129.7 kN for $t_f = 1.4$ mm. Both strip geometries exhibited relatively similar values concerning ductility index and strength factor.

When switching to the clearly higher CFRP cross-section 80 mm × 1.2 mm, due to the higher prestress force, the overall behavior under loading is obviously stiffer compared to the more narrow strip with b_f of 50 mm. When slabs SL50x1.2_MA and SL80x1.2_MA are compared (Figure 10c,e,) in terms of pull-out load at the end-anchorage, a higher force for the laminate with a higher cross-section can be deducted (see Figure 13). A strip width b_f of 80 mm results in an anchorage resistance of about 160 kN, whereas a more narrow laminate with $b_f = 50$ mm implicates a pull-out force of 126 kN. When comparing an average shear stress over the anchorage length of 270 mm the narrow strip delivers a higher strength than the larger one (9.16 MPa against 7.40 MPa). However, the CFRP strip with a higher axial stiffness might also implicate higher peak shear stresses at the anchorage tip (location where the laminate exits the anchorage zone towards midspan), being again responsible for an earlier strip pull-out. All in all, structural ductility is reduced when a higher CFRP cross-section is prestrained to the same level. Whereas relative force increases after yielding are rather similar for both cross-sections (SL50x1.2_MA and SL80x1.2_MA), clearly higher ductility indexes can be notived for the more slender strip. This behavior is analogue to classic prestressed concrete, for which a higher prestress level results in an enhanced cracking and yielding load, which eventually goes together with a reduced structural deformation capacity.

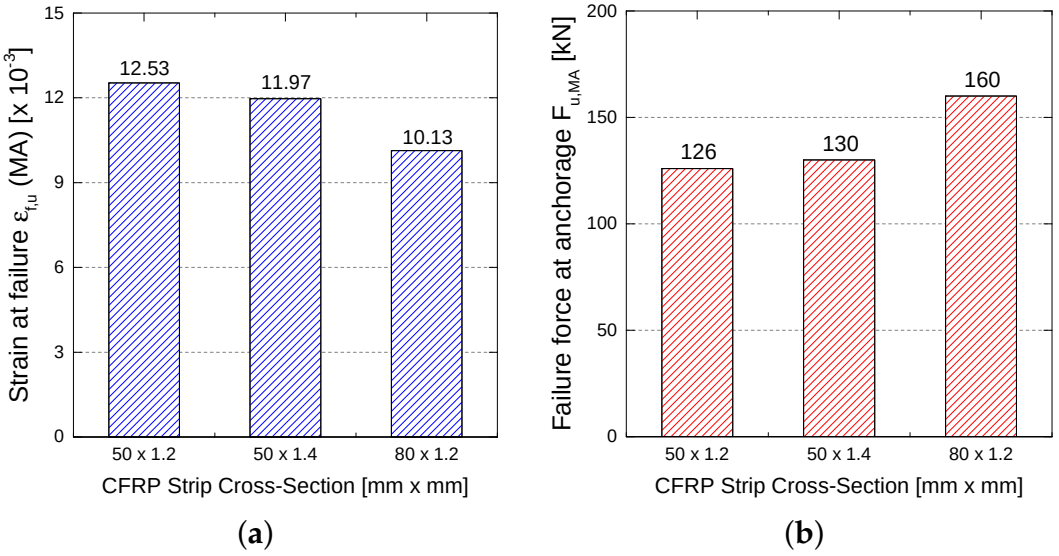

Figure 13. Measured CFRP tensile strain and deducted tensile force at pull-out. (**a**) CFRP tensile strain at failure; (**b**) CFRP force at failure.

4.6. Structural Behavior and Experiments/Simulation Comparison

Figure 10 presents the force-deflection predictions for the different configurations tested. In general, numerical predictions of the overall structural behavior fit well

with the experimental results obtained from the static loading tests. Regarding the reference tests, it has to be stated that the experiments were stopped at a midspan deflections of 100 mm due to the LVDT displacement range limitation. This explains the larger deflections at ultimate load carrying capacity for the numerical simulations. However, cracking, yielding and ultimate load along with the different stiffnesses are captured very well.

All retrofitted plates have been calculated up to theoretical tensile rupture of the CFRP strip or concrete crushing in compression. For the unstressed EBR configuration, again cracking and yielding load as well as the initial two pre- and postcracking stiffness are simulated in an accurate manner. Strip debonding occurred at a load of around 35 kN, corresponding to a strip tensile strain of 4.64‰. The simulated ultimate load is in this case somewhat higher at 44 kN with a tensile strain of the CFRP strip of 6.45‰. Failure is numerically governed by a debonding mode DM2, exceeding the interfacial shear stress.

For all tests with a prestressed CFRP strips, whether with a mechanical or a gradient anchorage, cracking and yielding loads together with the structural stiffness are again simulated quite precisely. Both configurations with a gradient anchorage eventually fail by strip debonding, which after an initiation rapidly propagates over the complete strip length. Numerically, the implemented debonding criteria as listed in Section 3.2 allow calculating the ultimate load in an accurate manner. Interesting observations can be made when analyzing the results of the slabs with a mechanical anchorage. For all specimens, strip debonding initiates on one side at a certain force level, followed by a progressive debonding over the complete strip length. Due to the mechanical end-anchorage, however, the CFRP strip does not becomes inactive, but acts eventually as an outer tension chord without any remaining bond to the concrete substrate but in both anchorage regions. This gradual transfer from a fully bonded to a finally unbonded system can be well observed by comparing the experimental results to both simulated cases. Up to the initiation of debonding, both the experimental curves coincide with the simulated bonded configuration. Afterwards, a gradual decrease in stiffness can be noticed up to failure by pulling the CFRP strip out of the mechanical anchorage. For both the strip sections of 50 mm $\times$ 1.2 mm and 50 mm $\times$ 1.4 mm, the structural behavior is finally almost identical to the one of a fully unbonded tendon, which can be well observed via the comparison between the experimental data and the simulated "unbonded" curve. Additionally, it can be noticed that the applied failure criteria (3) allows in these cases also predicting the ultimate load very closely.

5. Conclusions and Outlook

Out of the presented results, several conclusions can be drawn:

- As expected, clearly higher CFRP strains in tension can be reached with an initial prestressing.

- The type of anchorage for prestressed CFRP strips does not affect the behavior at serviceability. Cracking and immediate post-cracking structural behavior is identical for both techniques.
- The application of a gradient anchorage results in a more or less sudden strip debonding. The failure mode is very similar to conventional externally bonded reinforcement without any end-fixations.
- A mechanical end-anchorage system does also not prevent strip debonding, but allows to transfer the structural behavior from a bonded to an external unbonded-tendon-like behavior. The numerical simulations support this observation. Eventually, failure is obtained by pulling the CFRP strip out of the mechanical anchorage.
- In the present case, the application of a mechanical end-anchorage system implicated a much higher structural ductility when comparing the deflection at failure to the one at yielding. A gradient anchorage was not able to deliver the same amount of deformability.
- The implemented debonding criteria for conventional EBR reinforcements as well as the gradient failure criteria allow to re-calculate the slabs' behavior in an accurate manner. Future investigations, both experimental and numerical, shoud aim at defining precise pull-out resistances for mechanical anchorages.

Acknowledgments: This work is supported by FEDER funds through the Operational Program for Competitiveness Factors—COMPETE and National Funds through FCT—Portuguese Foundation for Science and Technology under the project FRPreDur-PTDC/ECM-EST/2424/2012. Additionally, the authors would like to thank all the companies that have been involved supporting and contributing for the development of this study, mainly: S&P Clever Reinforcement Ibérica Lda, S&P Clever Reinforcement Company (Switzerland), Tecnipor-Gomes & Taveira Lda., Vialam-Indústrias Metalúrgicas e Metalomecânicas, Lda., Hilti Portugal-Produtos e Serviços, Lda. The fourth author wishes also to acknowledge the grant SFRH/BD/98309/2013 provided by FCT. This paper is dedicated to Tiago Te[illegible]a (1988–2015), former doctoral student at the ISISE R&D Research Centre at the University of Min[illegible]

Author Contributions: Main Text Paragraph.

Conflicts of Interest: The authors declare no conflict of interest.

References

1. Bakis, C.; Bank, L.; Brown, V.; Cosenza, E.; Davalos, J.; Lesko, J.; Machida, A.; Rizkalla, S.; Triantafillou, T. Fiber-reinforced Polymer Composites for Construction—State-of-the-art Review. *J. Compos. Constr. (ASCE)* **2002**, *6*, 73–87.
2. SIA166. *Klebebewehrungen (Externally Bonded Reinforcements)*; SIA—Schweizer Ingenieur-und Architektenverein: Zürich, Switzerland, 2004; 40 page[illegible]
3. ISIS. *Strengthening Reinforced Concrete Structures with Externally-Bonded Fibre Reinforced Polymers*; The Canadian Network of Centres of Excellence on Intelligent Sensing for Innovative Structures (Canada[illegible]07.
4. ACI440.2R. *Guide for the Design and Construction of Externally Bonded FRP Systems for Strnegthening Concrete Structures*; American Concrete Institute: Farmington Hills, MI, USA, 2008; 80 pag[illegible]
5. HB305. *Design Handbook for RC Structures Retrofitted with FRP and Metal Plates: Beams and Slabs*; Standards Australia: Sydney, Australia, 2008; 80 page[illegible]
6. TR55. *Design Guidance for Strengthening Concrete Structures Using Fibre Composite Materials*; The Concrete Society (UK[illegible]012; 187 pages.

7. DAfStb. *Guideline—Strengthening of concrete members with adhesively bonded reinforcement*; Deutscher Ausschuss für Stahlbeton (DAfStb, Germany), 2012.
8. CNR. *Istruzioni per la Progettazione, l'Esecuzione ed il Controllo di Interventi di Consolidamento Statico Mediante L'utilizzo di Compositi Fibrorinforzati*; Consiglio nazionale delle ric[illegible]e (National Research Council)—Commissione di studio per la predisposizione e l'analisi (Italy), 2013; 144 page
9. Czaderski, C.; Motavalli, M. 40-Year-old full-scale concrete bridge girder strengthened with prestressed CFRP plates anchored using gradient method. *Compos. Part B: Eng.* **2007**, *38*, 878–886.
10. Motavalli, M.; Czaderski, C.; Pfyl-Lang, K. Prestressed CFRP for strengthening of reinforced concrete structures: Recent developments at Empa, Switzerland. *J. Compos. Constr. (ASCE)* **2011**, *15*, 194–205.
11. Wight, R.; Green, M.; Erki, M.A. Prestressed FRP sheets for poststrengthening reinforced concrete beams. *J. Compos. Constr. (ASCE)* **2001**, *5*, 214–220.
12. Svecova, D.; Razaqpur, A. Flexural behavior of concrete beams reinforced with carbon fiber-reinforced polymer CFRP prestressed prisms. *ACI Struct. J.* **2000**, *97*, 731–738.
13. Kim, Y.; Wight, R.; Green, M. Flexural strengthening of RC beams with prestressed CFRP sheets: Development of nonmetallic anchor systems. *J. Compos. Constr. (ASCE)* **2008**, *12*, 35–43.
14. Pellegrino, C.; Modena, C. Flexural strengthening of real-scale RC and PRC beams with end-anchored pretensioned FRP laminates. *ACI Struct. J.* **2009**, *106*, 319–328.
15. Michels, J.; Martinelli, E.; Czaderski, C.; Motavalli, M. Prestressed CFRP strips with gradient anchorage for structural concrete retrofitting: Experiments and numerical modeling. *polymers* **2014**, *6*, 114–131.
16. El-Hacha, R.; Wight, R.; Green, M. Prestressed fibre-reinforced polymer laminates for strengthening structures. *Prog. Struct. Eng. Mater.* **2001**, *3*, 111–121.
17. Michels, J.; Sena-Cruz, J.; Czaderski, C.; Motavalli, M. Structural strengthening with prestressed CFRP strips anchored with the gradient method. *J. Compos. Constr. (ASCE)* **2013**, *17*, 651–661.
18. LNEC. *Concrete—Determination of the Elasticity Young Modulus under Compression*; Portuguese specification from LNEC; LNEC-E397-1993; LNEC: Lisboa, Portugal, 1993.
19. IPQ—Instituto Português da Qualidada. *Testing Hardened Concrete—Part 3: Compressive Strength of Test Specimens*; NP-EN-12390-3; IPQ—Instituto Português da Qualidada: Caparica, Portugal, 2011.
20. IPQ—Instituto Português da Qualidada. *Metallic Materials. Tensile Testing. Part 1: Method of Test at Room Temperature*; NP-EN-ISO-6892-1; IPQ—Instituto Português da Qualidada, Caparica, Portugal, 2012.
21. ISO. *Plastics—Determination of Tensile Properties—Part 5: Test Conditions for Unidirectional Fibre-Reinforced Plastics*; ISO-527-5; ISO: Geneva, Switzerland, 2009.
22. ISO. *Plastics—Determination of Tensile Properties—Part 2: Test Conditions for Moulding and Extrusion Plastics*; ISO-527-2; ISO: Geneva, Switzerland, 1993.
23. Moussa, O.; Vassilopoulos, A.; de Castro, J.; Keller, T. Early-age tensile properties of structural epoxy adhesives subjected to low-temperature curing. *Int. J. Adhes. Adhes.* **2012**, *35*, 9–16.
24. Granja, J.; Fernandes, P.; Benedetti, A.; Azenha, M.; Sena-Cruz, J. Monitoring the early stiffness development in epoxy adhesives for structural strengthening. *J. Adhes. Adhes.* **2015**, *59*, 77–87.
25. Czaderski, C.; Martinelli, E.; Michels, J.; Motavalli, M. Effect of curing conditions on strength development in an epoxy resin for structural strengthening. *Compos. Part B: Eng.* **2012**, *43*, 398–410.
26. Michels, J.; Czaderski, C.; El-Hacha, R.; Brönnimann, R.; Motavalli, M. Temporary bond strength of partly cured epoxy adhesive for anchoring prestressed CFRP strips on concrete. *Compos. Struct.* **2012**, *94*, 2667–2676.
27. Marti, P.; Alvarez, M.; Kaufmann, W.; Sigrist, V. Tension chord model for structural concrete. *Struct.l Eng. Int.* **1999**, *115*, 832–838.
28. Harmanci, Y. Prestressed CFRP for structural retrofitting-experimental and analytical investigation. Master' Thesis. ETH Zurich, Switzerland, 2013.

29. Harmanci, Y.; Michels, J.; Czaderski, C.; Motavalli, M. Calculation technique for externally unbonded CFRP strips in structural concrete retrofitting. *J. Eng. Mech. (ASCE)* **2015**, doi:10.1061/(ASCE)EM.1943–7889.0001014, accepted manuscript.
30. Hognestad, E. A study of combined bending and axial load in reinforced concrete members. *Univ. Ill. Eng. Exp. Station—Bull. Ser.* **1951**, *399*, 128.
31. Czaderski, C. *Strengthening of Reinforced Concrete Members by Prestressed Externally Bonded Reinforcement with Gradient Method*. Ph. D. Thesis, No. 2052, ETH Zürich, Zürich, Switzerland, 2012; 459 pages, doi:10.3929/ethz-a-007569614.
32. Suter, R.; Jungo, D. Vorgespannte CFK-Lamellen zur Verstärkung von Bauwerken. *Beton Stahlbetonbau* **2001**, *96*, 350–358.
33. Harmanci, Y. *Externally Bonded Reinforcement EBR for Flexural Strengthening of Reinforced Concrete Beams with Rectangular Cross Section*; Semester Project, ETH Zürich, Zürich, Switzerland, 2011.